Electrospun PEG–PLA Nanofibrous Membrane for Sustained Release of Hydrophilic Antibiotics

Xiuling Xu,[1] Wen Zhong,[1,2] Shufei Zhou,[1] Adriana Trajtman,[2] Michelle Alfa[2]

[1]*Department of Textile Sciences, Faculty of Human Ecology, University of Manitoba, Winnipeg, Manitoba R3T 2N2, Canada*
[2]*Department of Medical Microbiology, Faculty of Medicine, University of Manitoba, Winnipeg, Manitoba R3T 2N2, Canada*

Received 7 May 2009; accepted 9 March 2010
DOI 10.1002/app.32415
Published online 21 May 2010 in Wiley InterScience (www.interscience.wiley.com).

ABSTRACT: Reported in this study is the successful incorporation of a hydrophilic antibiotic drug, tetracycline hydrochloride (TCH), into electrospun PEG–PLA nanofibrous membrane without loss of its bioactivity. Degradation behavior of the copolymer was studied *in vitro*. Release behavior of TCH from the electrospun membrane and antimicrobial effects of the TCH-loaded membrane against *Staphylococcus aureus* culture were investigated. The medicated nanofibrous membrane demonstrated sustained release of TCH over 6 days and was found to be effective in inhibiting growth of *S. aureus*. In addition, increasing the antibiotic drug content in the electrospun membranes was found to enhance the anti-bacterial effectiveness of the medicated fiber mats. And the combination of mechanical barriers provided by the electrospun biodegradable nanofibrous membranes and their capability of local sustained delivery of antibiotics made these membranes more useful in biomedical applications, particularly as new wound dressings for ulcers caused by diabetes or other diseases, and to provide a better means of treatment for these malignant wounds and ulcers. © 2010 Wiley Periodicals, Inc. J Appl Polym Sci 118: 588–595, 2010

Key words: electrospun; nanofibers; sustained release; antibiotics

INTRODUCTION

Major medical, social, and economic implications result from lower extremity amputation, a complication of diabetic foot ulcers.[1–4] It has been reported that approximately 15% of diabetics develop foot ulcers; non-healing ulcers precede 84% of all lower extremity amputations in diabetic patients.[1]

Diabetic foot ulcers are open wounds easily infected by bacterial contamination. Guidelines for treating these ulcers suggest that suitable dressings combining debridement and antimicrobial activity with moisture control are essential topical treatment methods.[3] Some of the dressings currently used in the treatment of skin ulcers may cause tissue damage through shear, friction, and/or pressure to the wound[5]; however, wound coverage is important to help prevent infection, and to treat infected ulcers.[6] Although antibiotics are useful in controlling infection, systemic administration can cause undesirable side effects including renal and liver toxicity,[6,7] can often provide insufficient dosage to the wounded tissues,[6] and can barely penetrate ischemic wounds with little granulation tissue. An effective treatment to overcome these side effects is topical administration,[6,8,9] in which the antibiotic is used in minimal amounts at the site of infection, and efforts are made to ensure that the drugs function efficiently at the site.

The rate of drug uptake by the human body may increase with the decrease in the size of the drug and its carrier, because of the increasing surface area of the drug or carrier. Hence, drug delivery systems have been developed using polymeric materials in the form of nano or micro particles,[10] hydrogels,[11] or micelles.[12] Recently, drug-loaded electrospun nanofibers have attracted a great deal of attention, because they offer higher drug encapsulation efficiency and better structural stability than other drug carriers.[13–15] Electrospinning is a simple method of fabricating nanofiber mats. A polymer solution is placed into a syringe with a capillary outlet and is subjected to a high voltage electric field. When the electric force exceeds the surface tension of the polymer solution, a fiber jet is ejected from the outlet. As the jet travels through the air, the solvent evaporates, leaving behind ultra-fine fibers that deposit on a grounded collector. Electrospun nanofibrous mats have a high porosity and a large specific surface area and could be used in the development of drug-loaded dressings that would allow sustained, site-

Correspondence to: W. Zhong (zhong@cc.umanitoba.ca).
Contract grant sponsors: NSERC (Natural Sciences and Engineering Research Council of Canada), MHRC (Manitoba Health Research Council).

specific delivery of drugs to wounds, while providing comfort by minimizing shear/friction to the wounded area.

Usually the physical and chemical properties of different drugs affect the success of incorporating them into nanofibers. Specifically, hydrophobic drugs can be easily encapsulated into hydrophobic polymers by electrospinning the mixed solution of a drug and a polymer. However, water-soluble drugs, including the commonly used broad-spectrum antibiotics such as clindamycin, cephalexin, ciprofloxacin, and cefoxitin sodium, cannot be directly incorporated into hydrophobic polymers. Although hydrophilic polymers are good carriers for water-soluble drugs, they cannot be used as the drug delivery system, because they can quickly dissolve in blood or tissue fluid. Under such conditions, the drug release rate cannot be controlled. Usually, the problem is solved by cross-linking the drug-loaded fibers.[16] However, many drugs may lose their bioactivity or even their molecular identity during cross-linking. Moreover, toxic chemicals may become incorporated into the dressings during the chemical cross-linking process.

Because of the difficulties as described above, only a few existing reports on electrospun fibrous mats for wound dressings[17–21] are devoted to developing dressings loaded with anti-infection drugs.[22] The aim of this work is, therefore, to develop electrospun drug-loaded fibrous dressings that will provide a locally-controlled release of drugs to the wounds. Specifically, the current study (1) involves a novel "emulsion-electrospinning" process to efficiently incorporate a hydrophilic antibiotic drug into the electrospun fibers without losing drug bioactivity and (2) is designed to demonstrate sustained release of the drug from the electrospun fibrous dressing, as well as its ability to inhibit bacterial growth. The work is expected to contribute to the development of new wound dressings for ulcers caused by diabetes or other diseases and to provide a better means of treatment for these malignant wounds and ulcers.

In the present study, TCH, a well-known broad spectrum antibiotic, is chosen as a model drug, because it is active against most common pathogens and will cause only a few allergic reactions.[23] The electrospun fibers of amphiphilic poly(ethylene glycol)-poly(L-lactic acid) (PEG–PLA) diblock copolymer are employed as vehicles for the release of this antibiotic. The viability and bioactivity of the released drug is examined using *in vitro Staphylococcus aureus* inhibition tests.

Wound dressings based on biodegradable PLA are promising for clinical uses, because the acidic environment induced by the degradation of the polymer helps to reduce bacteria growth[24,25] and promote epithelization.[25,26] Furthermore, it is reported that local lactate concentrations can stimulate local collagen synthesis.[25,27]

EXPERIMENTAL

Materials

Tetracycline hydrochloride (TCH, ≥95% purity), Fluorescein isothiocyanate (FITC), Polylactide (PLA) were purchased from Sigma-Aldrich Canada (Oakville, Ontario). Chloroform (analytical grade) was supplied by Fisher Scientific Canada (Ottawa, Ontario). Tris(hydroxymethyl) aminomethane (Tris-base) was supplied by Sigma-Aldrich, Canada and was used without further purification to prepare Tris-HCl buffer solution of pH = 8.6. Triethyl benzyl ammonium chloride (TEBAC), proteinase K and sodium azide were also purchased from Sigma-Aldrich, Canada. All reagents were used without further purification.

Diblock copolymer PEG–PLA (prepared from MPEG750 and L-lactide with a feed ratio of 17 : 620) was synthesized in our own lab. In a typical preparation process, L-lactide (supplied by Purac biomaterials, Lincolnshire, IL) was polymerized at 125°C with 0.025% w/w tin(II) octoate ($Sn(Oct)_2$) as catalyst and in the presence of PEG (supplied by Sigma-Aldrich Canada) as macromolecular initiator under argon atmosphere and anhydrous condition for 50 h. Then the polymerization product was dissolved in chloroform, precipitated into anhydrous alcohol, and dried in a vacuum at 60°C for 48 h. Dried PEG–PLA diblock copolymer is then obtained. Its molecular weight (M_n) and polydispersity (PD) determined by gel permeation chromatography (WATERS 410 GPC, Tetrahydrofuran was used as solvent with 1 mL/min flow rate, polystyrene as column standard) were 93,000 and 1.65, respectively.

Preparation and evaluation of water-in-oil emulsions containing TCH

The method to prepare water-in-oil (W/O) emulsions was described in detail by Xu, et al.[28] In the present study, two batches of 1 mL water solution containing, respectively, 1.0 and 3% w/w of TCH (with respect to PEG–PLA) were emulsified in 20 mL of 7.5% w/w chloroform solution of PEG–PLA in a Silverson L4RTA homogenizer. The homogenizer rotated at ~ 7000 r/min for about 20 min. To obtain stable and homogeneous W/O emulsions, 5% w/w of TEBAC (with respect to PEG–PLA) was added as a surfactant to the oily phase prior to emulsification, to lower surface tension and to render the aqueous emulsion droplets evenly distributed.

The zero shear viscosities and electrical conductivities of the as-prepared TCH containing emulsions and PEG–PLA control solution were measured at 25°C by a digital Viscometer (Brookfield DV-II+ PRO Digital Viscometer) and a conductivity meter (Orion 4-Star pH/Conductivity Benchtop Meter), respectively.

Preparation of TCH-loaded electrospun fibrous mats

The stable and homogenous W/O emulsions were electrospun using a conventional electrospinning setup. In the present study, electrospinning parameters were: electric field strength: 1.5–2.0 kV/cm; air gap distance: 20 cm; inner diameter of spinneret: 0.4 mm; flow rate of solution: 6–8 mL/h. In our experience, the optimal concentration of the PEG–PLA/chloroform solution was 7.5% w/w. Accordingly, this concentration was chosen throughout the electrospinning process in the study. In addition, electrospinning parameters were kept constant, and the experiment was conducted consistently at room temperature in air. To remove the residual chloroform, fiber mats collected were freeze-dried for about 48 h at −50°C under a vacuum of 10 Pa.

As a control, the unloaded PEG–PLA fibers were prepared by electrospinning 7.5% w/w chloroform solution of PEG–PLA. 5% w/w of TEBAC (with respect to PEG–PLA) was added into the PEG–PLA/CHCl3 solutions as a surfactant to improve the electrospinning process. The spinning parameters were all kept identical with those mentioned above.

A scanning electron microscope (SEM, Cambridge Stereoscan 120) was used to observe the surface morphology and size distribution of the electrospun fibers. Its accelerating voltage was 20 kV. Samples were mounted on metal stubs using a double-sided adhesive tape and vacuum-coated with a platinum layer prior to examination. To determine the average fiber diameter for each sample, 10 fibers from each sample were randomly selected in the SEM images, and fiber diameters were measured at six different points on each fiber.

Preparation of FITC-loaded electrospun fiber mats

To demonstrate the structure of the drug-loaded nanofibers fabricated by the emulsion electrospinning, FITC was used as an indicator (in place of TCH) in the emulsion electrospining as described in the previous sections. The distribution of FITC in the nanofibers was investigated under a confocal microscope (Olympus IX-70) with Fluoview Software using an Argon laser for excitation at 488 nm (green fluorescence).

In vitro degradation studies

For *in vitro* degradation studies, as-spun PEG–PLA and PLA fiber mats with a thickness of about 0.2–0.3 mm were cut into 20 × 20 mm^2 pieces. They were weighed (m_0), put into vials ($n = 3$) containing 25 mL of phosphate buffer solution (PBS, pH 7.4), and then incubated in a rotary shaker at 37 ± 0.1°C for various periods of time. At each specific incubation time, the samples were withdrawn and washed thoroughly with distilled water. The samples were wiped and dried in vacuum at room temperature until a constant weight (m_d) is obtained. The mass loss of the samples was calculated with the following equations:

$$\text{Mass loss percentage} = (m_0 - m_d)/m_0 \times 100$$

Degradation profiles of PEG–PLA and PLA fiber mats in the presence of an enzyme were obtained by putting samples in 0.05 mol/L Tris-HCl buffer solution (pH 8.6) containing 6μg/mL of proteinase K at 37 ± 0.1°C, following the same procedure as mentioned above.

It should be noted that PLA fiber mats were employed as a reference for the discussion of PEG–PLA degradation behavior. Its molecular weight (M_n) and polydispersity (PD) determined by gel permeation chromatography were 102,000 and 1.23, respectively.

In vitro drug release studies

The released TCH in the buffer solution was monitored by a UV-visible spectrophotometer at the wavelength of 366 nm. The drug-loaded fiber sample (20–30 mg) was incubated at 37°C in 20 mL of phosphate buffered saline (PBS, pH 7.4). At the required incubation time, the sample was transferred to 20 mL of fresh buffer solution, and the released TCH in the original buffer solution was determined. The detected UV absorbance of TCH was converted to its concentration according to the calibration curve of TCH in the same buffer. Then the accumulative weight and relative percentage of the released TCH were calculated as a function of incubation time.

The total content of TCH in the fibers was determined as follows. The three original TCH-loaded fiber mats were placed into separate vials filled with 20 mL of 0.05 mol/L Tris-HCl buffer solution (pH 8.6) containing 50μg/mL of proteinase K at 37°C. After about 5 h, the fiber mats were found to have all degraded into small chippings with the dimensions of the order of micros suspending in the buffer solution. We assumed that TCH had been completely released into the buffer solution. The cloudy

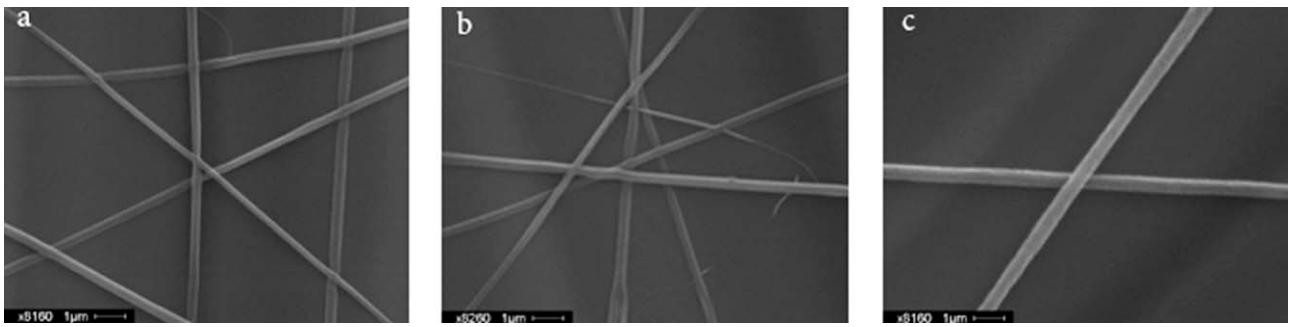

Figure 1 SEM images of 1% w/w (a) and 3% w/w (b) TCH-loaded PEG–PLA nanofibers and PEG–PLA nanofibers without drugs (c).

suspensions were filtered using 0.45 μm filter. Then the resultant solutions were monitored at the wavelength of 366 nm. Concentrations of released TCH in the solutions were determined according to the calibration curve of TCH in the same buffer. The total content of TCH in the fibers was easily calculated from the average of the three fiber mats. All results are expressed as the mean ± SD (standard deviation of the mean).

Antibiotic activities of TCH-loaded nanofibrous membranes

A modified Kirby-Bauer antibiotic test was used to assess the susceptibility of bacteria to drug-loaded nanofibrous membranes. A commercially available TCH-sensitive bacteria, *S. aureus* ATCC 25,923 (American Type Culture Collection, Seattle), was used for this test. In this study, the tested samples were divided into four groups: (1) a 1% w/w TCH-loaded fibrous disk (30 ug/disk), (2) a commercially available TCH-containing paper disk (30 ug/disk) (Antimicrobial Susceptibility Discs, Oxoid, Canada), (3) a TCH-loaded filter paper disk (30 ug/disk), prepared by means of dropping a TCH water solution onto a filter paper disk, and (4) negative controls: a blank PEG–PLA fibrous disks and a blank filter paper disk (without TCH). All samples were round disks of 0.6 cm in diameter. They are sterilized using UV irradiation before the susceptibility test.

The sample disks were placed on agar plates streaked with *S. aureus* suspension and incubated in a CO_2 incubator at 37°C. After 24 h, the inhibitory effect of each sample disk was evaluated by the diameter of an area of clearing around a disk where bacteria are not capable of growing (known as the inhibition zone). Then each sample disk was transferred to a fresh bacterial-streaked agar plate for the examination of the inhibitory effect provided by the remaining drug in the disk. Each test of antibacterial activity of the sample disks against *S. aureus* was performed for five consecutive days. The antibacterial experiments were performed in triplicate. The size of inhibition zone of each tested sample was measured and averaged from three different trials. All results are expressed as the mean ± SD (standard deviation of the mean). Student *t*-test is used to determine the significant differences among the groups. A P value less than 0.05 is considered to be significant.

RESULTS AND DISCUSSIONS

The morphology of the electrospun TCH-loaded PEG–PLA nanofibers with 1.0, and 3.0 w/w of TCH loadings is shown in Figure 1(a,b). They appeared uniform. Their surfaces were smooth and no drug crystals were detected. Moreover, it seemed that there were no significant differences in either the morphology or the average diameter of the composite fibers containing different amounts of tetracycline. Compared with unloaded PEG–PLA fibers [in Fig. 1(c)], they looked much thinner. Their average diameters were all about 600 nm, while the average diameter of unloaded PEG–PLA fibers was about 730 nm. This was ascribed to the decreasing viscosity of TCH containing emulsions due to high shear stress of homogenizer during emulsification process. The viscosities of the W/O emulsions containing 1.0 and 3.0 w/w of TCH and PEG–PLA blank solution were 0.53, 0.51, and 0.62 Pa s, respectively. Another possible reason for the reduction of the diameters of TCH-loaded PEG–PLA fibers was that the electrical conductivity of the spinning emulsion was enhanced because of the presence of TCH in the aqueous phase. The electrical conductivities of the W/O emulsions containing 1.0 and 3.0 w/w of TCH and PEG–PLA blank solution were 2.85, 2.94, and 3.12 S m^{-1}, respectively. Therefore, in the present study, both effects favor the formation of TCH-loaded fibers with smaller diameters.

A confocal microscope image for FITC-loaded PEG–PLA nanofiber that has been fabricated using the same method was shown in Figure 2. It can be seen from the image that the green fluorescent FITC has been trapped in the core of the nanofiber,

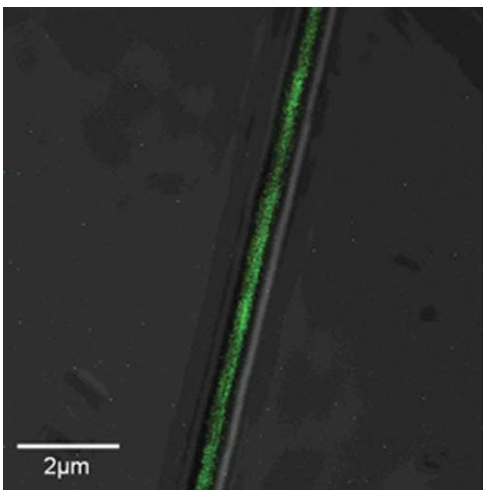

Figure 2 Confocal microscope image for FITC-loaded PEG–PLA nanofiber. [Color figure can be viewed in the online issue, which is available at www.interscience.wiley.com.]

demonstrating the formation of a sheath/core structure via the emulsion electrospinning, with small molecular drug in the core and polymer on the sheath of the nanofiber.

Degradation

The hydrolytic degradation of both PLA and PEG–PLA fiber mats was carried out in PBS at 37 ± 0.1°C. Their profiles of degradation were shown in curves a and b in Figure 3. It can be seen that the two polymers display similar degradation kinetics. In PBS, their rates of weight loss remained relatively low in the first 23 days. By the end of Day 23, the remaining masses of PLA and PEG–PLA fiber mats were 92.8 ± 1.5% and 87.4 ± 1.6%, respectively. Their rates of weight loss increased from Day 23 and raised dramatically from Day 56. By the end of Day 85, the remaining masses of PLA and PEG–PLA fiber mats reduced to 33.1 ± 4.0% and 14.7 ± 6.9%, respectively. It is known that the hydrolysis of PLA is a process in which ester bonds are randomly cut. The hydrolysis process can be further autocatalyzed by the carboxylic acid groups generated during degradation, especially by those carboxylic acid groups in the center of the fiber mass.[29–32] As a result, the degradation of PLA in PBS is heterogeneous with a fast degrading center and a slowly degrading outer layer.[29] It can be seen that the hydrolysis degradation rate of PEG–PLA fiber mats was faster than that of the PLA ones. The reason is that hydrophilic PEG blocks allow more water molecules to diffuse into the interior of the fibers.

The degradation of both PEG–PLA and PLA fiber mats was significantly accelerated in the presence of proteinase K (curves c and d in Fig. 3). In the presence of proteinase K, the mass losses of PEG–PLA and PLA fiber mats were 72.5 ± 3.9% and 89.8 ± 2.8%, respectively in only 1.8 days, if compared to their mass loss of 85.2 ± 4.0% and 66.9 ± 6.9%, respectively in 85 days in PBS. This was in agreement with the reports that proteinase K can catalyze the hydrolysis of PLA molecules.[33,34] Furthermore, in the presence of protainase K, the weight loss of both PEG–PLA and PLA fiber mats increased steadily with the degradation time (Fig. 3, inserted curves c and d), because the enzymatic degradation is mainly a surface erosion process. Similar degradation behavior was also shown in other reports,[35] which indicated that the enzymatic degradation itself of PLA electrospun fibers was of zero-order kinetics.

It was interesting to see that the enzymatic degradation rate of PEG–PLA fiber mat was slower than that of PLA fiber mat, although the former was more hydrophilic than the latter. For example, by the end of 1.3 h, 53.3 ± 2.2% and 68.2 ± 5.1% of mass loss were monitored for PEG–PLA and PLA, respectively. The interpretation is as follows: the enzymatic degradation takes place in two steps: (1) the enzyme approaches the fiber surface; (2) it initiates hydrolysis of the polymer. The second step is determined by the nature and concentration of the enzyme used, while the first step is determined by the surface properties of the fibers. It is possible that PEG blocks enriched on the surface of the PEG–PLA fibers, when PEG–PLA fibers contact with water. However, proper PEG chains can sterically prevent

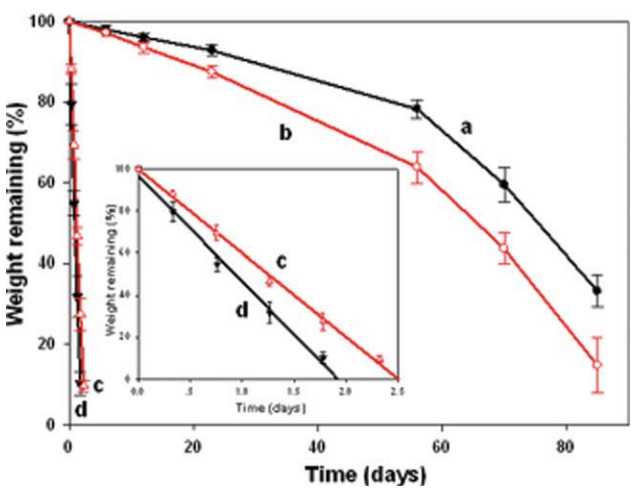

Figure 3 Weight remaining of PEG750–PLA (red curves, b and c) and PLA (black curves, a and d) polymers as a function of degradation time in PBS (-●- for PLA and -○- for PEG–PLA) and in 0.05 mol/L Tris-HCl buffer solution (pH 8.6) containing 6μg/mL of proteinase K (-▼- for PLA and -Δ- for PEG–PLA) at 37°C. The insert is the magnification of curves c and d. [Color figure can be viewed in the online issue, which is available at www.interscience.wiley.com.]

enzymatic attack to PLA molecules to some extent.[36,37]

The degradation behavior of PEG–PLA contacting with open wound *in vivo* will be studied in our future work.

Release of TCH from TCH-loaded nanofibers

Figure 4 shows the release profiles of TCH from 1 and 3% w/w TCH-loaded fiber mats, respectively. Both membranes showed a sustained drug release behavior, although a certain amount of rapid drug release was found within the first 12 h (32.5% for 1% w/w samples vs. 21.8% for 3% w/w samples) in comparison to the entire 6 days' release experiment. For the delivery of antibiotic drugs, a certain initial burst release is actually required to achieve enough initial dosage, because it is important to eliminate the intruding bacteria before they begin to proliferate. As for the bacteria cells that have survived the initial stage, sustained drug release is necessary to prevent their further population.[38] It was interesting to notice that rate of TCH release would decrease with increased TCH content in the fibers during the entire process of release. For example, the release percentages were about 47.8 and 34.4% at Day 1, 72.2 and 54.9% at Day 2, 83.0 and 70.3% at Day 3, respectively, for the two samples examined. Similar release behaviors were reported by Xu et al.[39] In an emulsion electrospinning, TCH was well incorporated into PEG–PLA fibers, forming core-sheath structured fibers (Fig. 2) during the electrospinning of the W/O emulsion containing TCH. This kind of core-sheath structured fibers is a reservoir-type drug-loaded system: a greater amount of TCH in the emulsion for electrospinning resulted in a thinner core and a thicker sheath of fibers due to the movement of TCH towards the fiber axis and the higher degree of de-emulsification of the aqueous droplet with larger TCH concentration. It was found in this study, however, rate of release from the 1% w/w TCH-loaded fibers was larger than that from the 3% w/w fibers. The difference of percentages of daily release from 3% w/w fibers was not as obvious as the difference of percentages of daily release from 1% w/w fibers [Fig. 4(B)], indicating that the 3% w/w fibers displayed more sustained release due to a smaller rate of release.

For both samples, daily release of TCH decreased gradually as the 6-day experiment approached its end [Fig. 4(B)]: about 47.8, 24.4, and 10.8% of TCH were released from 1% w/w TCH-loaded fibers within Days 1, 2, and 3, respectively, but only 3.5, 1.4, and 0.7% of TCH were released in Days 4, 5, and 6; likewise, release from 3% w/w TCH-loaded fibers were about 34.4, 20.5, and 15.4% in Days 1, 2, and 3, but only 6.7, 4.5, and 2.7% in Days 4, 5, and 6,

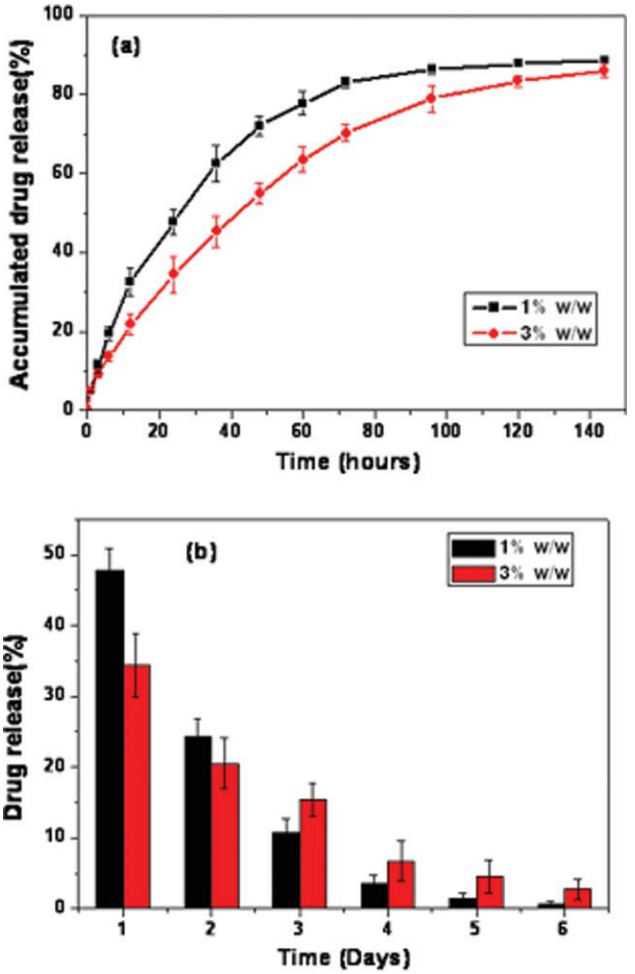

Figure 4 Profiles of the release of TCH from 1% w/w and 3% w/w TCH-loaded PEG–PLA nanofibers in PBS at 37°C, the data representing the mean ± SD ($n = 3$): cumulative curve (a) and differential curve (b). [Color figure can be viewed in the online issue, which is available at www.interscience.wiley.com.]

respectively. Interpretation can be as follows. First, TCH in the fibers runs out as the release goes on and on. Second, TCH molecules located in the center of the fibers have a longer distance to travel in the course of diffusing. Another reason is increased crystallinity of PEG–PLA as a result of its incubation in PBS at 37°C. It is known that a small molecule diffuses more slowly through a crystalline polymer than through an amorphous polymer of the same kind,[40] so that release of TCH slows down as the release goes on and on.

Antimicrobial activities of TCH-loaded nanofiber membranes

To evaluate the efficacy of the medicated membranes, in this study, use was made of a commercially available TCH-sensitive bacterium, a Gram-positive spherical bacterium that is typically found

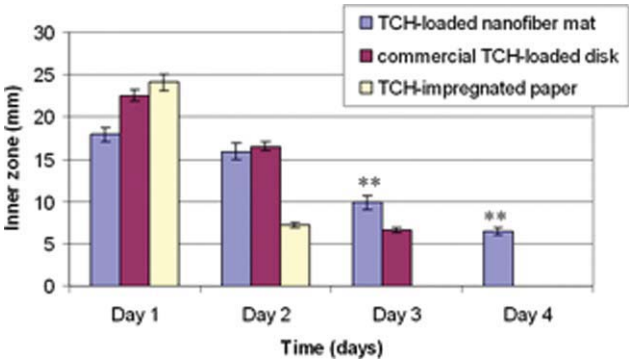

Figure 5 Diameters of inhibition zones in the *Staphylococcus aureus* susceptibility test (30 ug/disk for all samples). [Color figure can be viewed in the online issue, which is available at www.interscience.wiley.com.]

in the skin, nasal passages, and mucous membranes, and can cause a wide range of suppurative infections.[38] The antimicrobial effect of electrospun membranes with and without TCH can be compared by the sizes of their inhibitory zones. Besides, two positive controls, a commercial TCH-loaded disk and TCH-impregnated paper, were used to compare the sustained release of drugs from drug-loaded substrates. There was no inhibitory zone surrounding the negative control (drug-free electrospun fiber disk) on the bacterial-inoculated agar plate and bacteria grew robustly. The results of the microorganism susceptibility tests for all samples except the negative control were shown in Figure 5. It can be noted that obvious inhibitory zones were observed around the 1% w/w TCH-loaded fiber mats: average 17.9 mm for Day 1, 15.9 mm for Day 2, and 9.9 mm for Day 3, respectively. Although the zones of inhibition were much smaller (6.5 mm in average) at Day 4, but the inhibitory effects were still seen on that day in the antibiotic-containing disk. On Day 5, the released TCH was not enough to inhibit the bacteria, so the remaining viable bacteria could proliferate, and, as a result, no inhibition zone was observed at Day 5.

One the contrary, one of the positive control (TCH on the paper) gave the largest inhibition zone (24.1 mm) at Day 1, as shown in Figure 5, indicating that most of the TCH was released from the paper in the first day because of the burst release. At Day 2, its inhibitory effect decreased dramatically to 7.2 mm. From the third day, inhibition zone was not observed any longer, because almost all drugs had been depleted from the paper in the first two days.

As also demonstrated in Figure 5, the other positive control (commercial paper disk) had its inhibitory effect in the first 3 days, and diameters of the inhibitory zone decreased dramatically (22.5 mm at Day 1, 16.5 mm at Day 2, and 6.6 mm at Day 3). At Days 4 and 5, the commercial paper disk lost its antibacterial activity because the TCH had almost got depleted in the disk after 3 days' release.

Statistical analysis reveals that on Days 4 and 5, the effect of bacteria inhibition of TCH-loaded nanofibers is significantly higher than both the negative and positive controls ($P < 0.01$), as indicated in Figure 5. These results were enough to confirm that TCH released from the medicated membrane will retain its biological function, or that the activity of antibiotics will be preserved after emulsification and electrospinning. And prolonged inhibitory effects of TCH-loaded fiber mats on *S. aureus* indicated sustained release of TCH from the medicated membrane, which is consistent with data in Figure 4.

For a comparison with the 1% w/w TCH-loaded fiber mats, 3% w/w TCH-loaded fiber mats were tested to clarify how the anti-bacterial effectiveness of medicated fiber mats was related with increased TCH content in the electrospun membranes. Obviously, the latter had stronger and more sustained inhibitory effects on *S. aureus* (Fig. 6). Specifically, even at Day 5, release of bioactive drug from 3% w/w TCH-loaded fiber mat was still able to substantially inhibit bacterial growth, displaying a 12 mm inhibition zone on the agar plate; however, no inhibition zone was observed in the case of 1% w/w TCH-loaded fiber mat at that day (Fig. 6). In addition, the inhibition zone of 3% w/w TCH-loaded fiber mats vanished less quickly than that of the 1% w/w TCH-loaded fiber mats. These results are in agreement with what is shown in Figure 4: rate of release of TCH decreases with increased TCH content in the fibers, so that 3% w/w TCH-loaded fiber mats are capable of a more sustained TCH release than the 1% w/w TCH-loaded fiber mats. Statistical analysis also suggests that all the differences in bacteria inhibitions are significant ($P < 0.01$) except for Day 2.

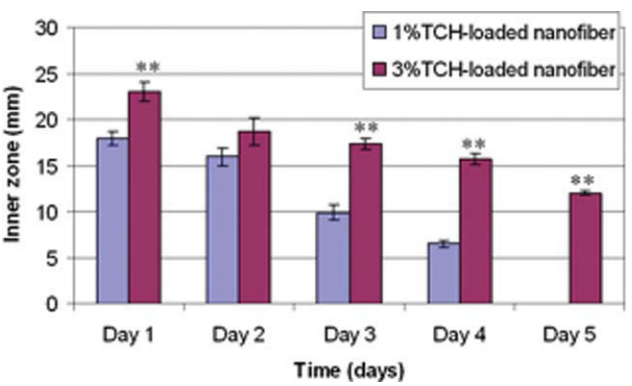

Figure 6 Diameters of inhibition zones in the *Staphylococcus aureus* susceptibility test of 1% w/w and 3% w/w TCH-loaded PEG–PLA fibrous mat. [Color figure can be viewed in the online issue, which is available at www.interscience.wiley.com.]

CONCLUSIONS

Medicated biodegradable PEG–PLA nanofibrous membranes containing TCH were fabricated by means of emulsion-electrospinning. *In vitro* degradation studies revealed that the PEG–PLA nanofiber mats showed an 85% mass loss by the end of 85 days in PBS. However, the presence of proteinase K significantly increased the degradation process, indicating the possibility of a different degradation profile *in vivo*, which will be studied in our future work. Successfully incorporated into the nanofibers and evenly released without losing its bioactivity, the drug proved to be effective in inhibiting *S. aureus* bacteria growth in 5 consecutive days. Increased TCH content in the electrospun membranes enhanced the anti-bacterial effectiveness of these medicated fiber mats and helped sustain the release. Our work is expected to lead to the development of new wound dressings that are capable of controlled release of therapeutic agents to prevent bacterial growth, and, as a result, to significantly reduce the costs of treatment and care of diabetic foot ulcers.

References

1. Mcintyre, I.; Boughen, C.; Trepman, E.; Embil, J. M. Foot Ankle Int 2007, 28, 674.
2. Reid, K. S.; Martin, B. D.; Duerksen, F.; Nicolle, L. E.; Garrett, M.; Simonsen, J. N.; Trepman, E.; Embil, J. M. Foot Ankle Int 2006, 27, 1065.
3. Steed, D. L.; Attinger, C.; Colaizzi, T.; Crossland, M.; Franz, M.; Harkless, L.; Johnson, A.; Moosa, H.; Robson, M.; Serena, T.; Sheehan, P.; Veves, A.; Wiersma-Bryant, L. Wound Repair Regen 2006, 14, 680.
4. Zhong, W.; Xing, M. M. Q.; Pan, N.; Maibach, H. I. Cutaneous Ocul Toxicol 2006, 25, 23.
5. Cochrane, C.; Rippon, M. G.; Rogers, A.; Walmsley, R.; Knottenbelt, D.; Bowler, P. Biomaterials 1999, 20, 1237.
6. Stadelmann, W. K.; Digenis, A. G.; Tobin, G. R. Am J Surg 1998, 176, 39s.
7. Suzuki, Y.; Tanihara, M.; Nishimura, Y.; Suzuki, K.; Kakimaru, Y.; Shimizu, Y. J Biomed Mater Res 1998, 42, 112.
8. Fallon, M. T.; Shafer, W.; Jacob, E. J Surg Res 1999, 86, 97.
9. Jacob, E.; Cierny, G.; Fallon, M. T.; Mcneill, J. F.; Siderys, G. S. J Orthop Res 1993, 11, 404.
10. Soppimath, K. S.; Liu, L. H.; Seow, W. Y.; Liu, S. Q.; Powell, R.; Chan, P.; Yang, Y. Y. Adv Funct Mater 2007, 17, 355.
11. Partap, S.; Muthutantri, A.; Rehman, I. U.; Davis, G. R.; Darr, J. A. J Mater Sci 2007, 42, 3502.
12. Torchilin, V. P. Pharm Res 2007, 24, 1.
13. Han, X. J.; Huang, Z. M.; He, C. L.; Liu, L. High Perform Polym 2007, 19, 147.
14. Kumbar, S. G.; Nair, L. S.; Bhattacharyya, S.; Laurencin, C. T. J Nanosci Nanotechnol 2006, 6, 2591.
15. Chew, S. Y.; Wen, Y.; Dzenis, Y.; Leong, K. W. Curr Pharm Des 2006, 12, 4751.
16. Goldberg, M.; Langer, R.; Jia, X. Q. J Biomater Sci Polym Ed 2007, 18, 241.
17. Venugopal, J.; Ramakrishna, S. Appl Biochem Biotechnol 2005, 125, 147.
18. Hinrichs, W. L. J.; Lommen, E. J. C. M. P.; Wildevuur, C. R. H.; Feijen, J. J Appl Biomater 1992, 3, 287.
19. Leipziger, L. S.; Glushko, V.; Dibernardo, B.; Shafaie, F.; Noble, J.; Nichols, J.; Alvarez, O. M. J Am Acad Dermatol 1985, 12, 409.
20. Khil, M. S.; Cha, D. I.; Kim, H. Y.; Kim, I. S.; Bhattarai, N. J Biomed Mater Res B Appl Biomater 2003, 67, 675.
21. Wang, L. H.; Khor, E.; Wee, A.; Lim, L. Y. J Biomed Mater Res 2002, 63, 610.
22. Kenawy, E. R.; Bowlin, G. L.; Mansfield, K.; Layman, J.; Simpson, D. G.; Sanders, E. H.; Wnek, G. E. J Control Release 2002, 81, 57.
23. Schnappinger, D.; Hillen, W. Arch Microbiol 1996, 165, 359.
24. Varghese, M. C.; Balin, A. K.; Carter, D. M.; Caldwell, D. Arch Dermatol 1986, 122, 52.
25. Zilberman, M.; Elsner, J. J. J Control Release 2008, 130, 202.
26. Eisinger, M.; Lee, J. S.; Hefton, J. M.; Darzynkiewicz, Z.; Chiao, J. W.; Deharven, E. Proc Natl Acad Sci USA 1979, 76, 5340.
27. Hutchinson, F. G.; Furr, B. J. A. Biochem Soc Trans 1985, 13, 520.
28. Xu, X. L.; Yang, L. X.; Xu, X. Y.; Wang, X.; Chen, X. S.; Liang, Q. Z.; Zeng, J.; Jing, X. B. J Control Release 2005, 108, 33.
29. Maquet, V.; Boccaccini, A. R.; Pravata, L.; Notingher, I.; Jerome, R. Biomaterials 2004, 25, 4185.
30. Kim, K.; Yu, M.; Zong, X. H.; Chiu, J.; Fang, D. F.; Seo, Y. S.; Hsiao, B. S.; Chu, B.; Hadjiargyrou, M. Biomaterials 2003, 24, 4977.
31. Li, S. M.; Mccarthy, S. Biomaterials 1999, 20, 35.
32. Li, S. M. J Biomed Mater Res 1999, 48, 342.
33. Li, S. M.; Mccarthy, S. Macromolecules 1999, 32, 4454.
34. Liu, L. J.; Li, S. M.; Garreau, H.; Vert, M. Biomacromolecules 2000, 1, 350.
35. Zeng, J.; Chen, X. S.; Liang, Q. Z.; Xu, X. L.; Jing, X. B. Macromol Biosci 2004, 4, 1118.
36. Mosqueira, V. C. F.; Legrand, P.; Morgat, J. L.; Vert, M.; Mysiakine, E.; Gref, R.; Devissaguet, J. P.; Barratt, G. Pharm Res 2001, 18, 1411.
37. Kushibiki, T.; Matsuoka, H.; Tabata, Y. Biomacromolecules 2004, 5, 202.
38. Kim, K.; Luu, Y. K.; Chang, C.; Fang, D. F.; Hsiao, B. S.; Chu, B.; Hadjiargyrou, M. J Control Release 2004, 98, 47.
39. Xu, X. L.; Zhuang, X. L.; Chen, X. S.; Wang, X. R.; Yang, L. X.; Jing, X. B. Macromol Rapid Commun 2006, 27, 1637.
40. Miyajima, M.; Koshika, A.; Okada, J.; Ikeda, M.; Nishimura, K. J Control Release 1997, 49, 207.